Cell Death and Differentiation (2008) 15, 283–298

www.nature.com/cdd

Identification of new kinase clusters required for neurite outgrowth and retraction by a loss-of-function RNA interference screen

SHY Loh[1], L Francescut[1], P Lingor[2,3], M Bähr[2,3] and P Nicotera*[,1]

Disruption of synaptic integrity, loss of connectivity and axodendritic degeneration are early and essential components of neurodegeneration. Although neuronal cell death mechanisms have been thoroughly investigated, less is known about the signals involved in axodendritic damage and the processes involved in regeneration. Here we conducted a genome-wide RNA interference-based forward genetic screen, using small interfering RNA targeting all human kinases, and identified clusters of kinases families essential for growth cone collapse, neurite retraction and neurite outgrowth. Of 59 kinases identified as positive regulators of neurite outgrowth, almost 50% were in the tyrosine kinase/tyrosine kinase-like (TK/TKL) receptor subgroups, underlining the importance of extracellular ligands in this process. Neurite outgrowth was inhibited by 66 other kinases, none of which were TK/TKL members, whereas 79 kinases inhibited lysophosphatidic acid-induced neurite retraction. Twenty kinases were involved in both inhibitory processes suggesting shared mechanisms. Within this group of 20 kinases, some (ULK1, PDK1, MAP4K4) have been implicated previously in axonal events, but others (MAST2, FASTK, CKM and DGUOK) have not. For a subset of kinases, the effect on neurite outgrowth was validated in rat primary cerebellar cultures. The ability to affect regeneration was further tested in a model of axodendritic lesion using primary rat midbrain cultures. Finally, we demonstrated that haploinsufficiency of two members of the AGC kinase subgroup, ROCK1 and PKN1, was able to suppress retinal degeneration in *Drosophila* model of class III Autosomal Dominant Retinitis Pigmentosa.
Cell Death and Differentiation (2008) **15,** 283–298; doi:10.1038/sj.cdd.4402258; published online 16 November 2007

Neurodegenerative diseases, such as Alzheimer's, Parkinson's and Huntington's, are characterized by neuronal degeneration in the central nervous system (CNS). Research efforts have focused mainly on neuronal demise, of which apoptosis, necrosis and autophagic death of the neuronal soma are the most commonly described.[1] On the contrary, the disruption of synaptic integrity, loss of connectivity and axonal degeneration which often precede, and are not always associated with, neuronal demise have not been thoroughly addressed. Although the mechanisms leading to axonal degeneration are largely unknown, there is compelling evidence that different execution systems operate in the axons and in the soma during neuronal degeneration.[2–4] Selective, localized processes are also critical for neurite sprouting, axon growth, extension of the dendritic tree and establishment of precise connections with specific target cells. These are active during neuronal development, but they are also important for neuronal plasticity, as well as neuronal regeneration after damage to neurites and nerve endings.

Processes of both neuronal degeneration and regeneration involve complex signalling cascades leading to remodelling of cytoskeletal architecture, changes in ion signalling and mitochondrial function and distribution. Several signalling cascades involved in neurodegenerative/regenerative processes involve protein phosphorylation by kinases.[5,6] Aberrantly active protein kinases have been implicated in a variety of disease states, including neurodegenerative disorders[7,8] and kinases are directly responsible for some of the most characteristic neuronal alterations in neurodegeneration. For example, CDK5 and GSK3β regulate hyperphosphorylation of the microtubule-associated protein tau and formation of intraneuronal neurofibrillary tangles (NFTs) in Alzheimer's disease (AD) patients.[9,10] Overexpression of CDK5 and GSK3β in neuronal cultures and transgenic animal models not only leads to tau phosphorylation but also causes cytoskeletal structural abnormalities and neurodegeneration.[11] Recent studies indicate that the genes encoding the PINK1 and LRRK2 protein kinases are mutated in patients with early and late onset Parkinson's disease, respectively[12–16] and work in *Drosophila melanogaster* has provided further evidence of the role of mutant PINK1 in mitochondria dysfunction and cell death.[17] Altered kinase activity is essential for the neurodegenerative effects of mutant PINK1 and LRRK2. Pathogenic mutants and kinase-dead PINK1 abrogate the neuroprotective effect of wild-type PINK1,[18] whereas pathogenic mutations in LRRK2 increase its kinase

[1]MRC Toxicology Unit, University of Leicester, Leicester, UK; [2]Department of Neurology, Georg-August-University Göttingen, Faculty of Medicine, Waldweg 33, Göttingen, Germany and [3]DFG-Research Center for Molecular Physiology of the Brain (CMPB), Göttingen, Germany
*Corresponding author: P Nicotera, MRC Toxicology Unit, Hodgkin Building, Lancaster Road, Leicester, LE1 9HN, UK. Tel: + 44 1162525611; Fax: + 44 1162525599; E-mail: pn10@le.ac.uk
Keywords: RNAi screen; human kinases; neurite outgrowth; neurite retraction
Abbreviations: AD, Alzheimer's disease; CNS, central nervous system; CGN, cerebellar granule neurons; DIV, days *in vitro*; db-cAMP, dibutyryl-cyclic AMP; EGFP, enhanced green fluorescent protein; GFP, green fluorescent protein; LPA, lysophosphatidic acid; mtDNA, mitochondrial DNA; PKA, protein kinase A; PKG, protein kinase G; PKC, protein kinase C; RNAi, RNA interference; siRNA, small interfering RNA; TK/TKL, tyrosine kinase/tyrosine kinase-like
Received 23.7.07; revised 21.9.07; accepted 24.9.07; Edited by G Melino; published online 16.11.07

activity, and cause neurodegeneration in neuronal cultures.[19–22] Several other kinases, such as members of the casein kinases family (CK1δ, CK1α) and DYRK1A, have also been implicated in tauopathies such as AD, based on their abilities to phosphorylate tau, as well as β-secretase and presenilin, two other proteins linked to AD.[23,24]

Despite the enormous research focus on individual pathways involving kinase regulation in neurodegenerative disorders, the underlying consequences of a disturbed signalling machinery are still obscure. Most importantly, although the position of individual kinases in signal transduction is well established in many cases, there is no comprehensive picture of the overall cross-talk between kinase families in pathophysiological processes. To address this complexity, we designed an RNA interference (RNAi)-based forward genetic screen, using small interfering RNA (siRNA) targeting the majority of human kinases, with the aim of identifying clusters of kinases essential for growth cone collapse, neurite retraction and neurite outgrowth. In addition to unraveling the complex interactions between different kinase families, this study has also uncovered novel roles for kinases that have not yet been assigned a function or have not previously been implicated in neuronal function. This may foster new understanding of mechanisms involved in neurodegeneration and help in designing effective and non-toxic treatments based on modulation of different kinase subsets.

Results

High-throughput screen of human kinases involved in neurite outgrowth. To establish the role of protein kinases in neurite outgrowth and retraction, we designed a functional assay using the human neuroblastoma cell line, SH-SY5Y. In the presence of dibutyryl-cyclic AMP (db-cAMP), SH-SY5Y cells form elongated β-III tubulin-immunopositive processes within 48 h (Figure 1a and b). The average neurite length per neuron (ANL/neuron) for non-differentiated and differentiated cells was 40–50 and 70–80 μm, respectively (Figure 1e). SH-SY5Y cells were then systematically transfected with siRNAs using a kinome library comprising 750 kinases at three-fold redundancy. Cells were then differentiated in medium containing db-cAMP (Supplementary Figure 1). Under these conditions, more than 92% of cells were transfected with siRNA (Supplementary Figure 2). As selection criterion, we used neurite length and considered a kinase to be genuine when two or more siRNA against the same candidate kinase produced the same phenotype (low or high ANL/neuron). Because undifferentiated SH-SY5Y cells undergo cell division, siRNAs to some kinases also affected their proliferation rate and thereby might have affected only indirectly their neurite outgrowth (Figure 1g). However, some cell cycle kinases were also involved in neurite outgrowth suggesting possible new functions for this kinase family. After two rounds of stringent analyses, siRNAs (two or more) that increase the ANL/neuron to $>100\,\mu$m were defined as promoting neurite outgrowth and those that decrease the ANL/neuron to $<70\,\mu$m were defined as inhibiting neurite outgrowth (Figure 1f).

High-throughput screen of human kinases involved in neurite retraction. In the neurite retraction assay, db-cAMP-differentiated cells were treated with lysophosphatidic acid (LPA) for 1 h to induce growth cone collapse and neurite retraction (Figure 2b). As a positive control, we used siRNA to *Rock1*, which is known to inhibit these processes (Katoh *et al*.[25] and Figure 2c). In addition, LPA induction also caused the cell body to flatten (Figure 2b and c). In this screen, the ANL/neurite for differentiated cells with or without LPA induction was 10.18 and 13.58 μm, respectively (Figure 2g). As for the outgrowth screen, the entire retraction screen was repeated and an average of both experiments were analysed. siRNAs (two or more) that maintained ANL/neurite to $>12\,\mu$m were defined as inhibiting LPA-induced neurite retraction (Figure 2h).

Analysis of the screen data. Our analysis revealed that siRNA-targeted downregulation of $\sim$8% (59 candidates) of the kinome library resulted in neuronal cells exhibiting short neurite length (Table 1). In the case of 13 kinases, neurite outgrowth was inhibited by all three independent siRNAs. The efficiency of downregulation by all three siRNAs for four candidates (SNARK1, EPHA1, ERBB2 and JAK1) was further confirmed by quantitative RT-PCR (Supplementary Figure 3). Interestingly, inhibition of neurite outgrowth by LIMK1 was observed from only two independent siRNAs and this was due to an inefficient downregulation by the third siRNA (Supplementary Figure 3). Targeted downregulation of another 9% (66) kinases resulted in cells with abnormally long neurite length (Table 2). In the case of 15 kinases, neurite outgrowth was promoted by all three independent siRNAs.

The processes of growth cone collapse and neurite retraction induced by LPA were inhibited by 79 kinases. Interestingly, 20 of these kinases were identical to those which inhibited neurite outgrowth (Table 3 and Figure 3), suggesting a shared mechanism in the inhibition of outgrowth and retraction. The kinases identified in all three data sets are clustered in the kinome (http://kinase.com). The majority (50%) of the positive modulators of neurite outgrowth (inhibitory candidates) belong to the tyrosine kinase (TK) and tyrosine kinase-like (TKL) subgroups (Table 1 and Figure 3). This finding suggests that neurite outgrowth is promoted primarily by extracellular ligands and growth factors and suggests that this subset of kinases could be a potential target for therapeutic intervention. However, on the contrary, most of the negative modulators (stimulatory candidates) of neurite outgrowth are from the AGC (containing protein kinase A (PKA), protein kinase G (PKG), protein kinase C (PKC) families) subgroup and no TK/TKL kinases are involved in this process (Table 2 and Figure 3). Promotion and inhibition of neurite outgrowth required signalling from different subgroups of kinase families. Our results also revealed that the control of neurite length required a balance of cellular signals that both promotes and restricts neurite outgrowth. By contrast, no kinases that promote neurite outgrowth were involved in LPA-induced neurite retraction. The 27 TK/TKL-positive modulators of neurite outgrowth were different from the 19 TK/TKL kinases involved in the retraction, suggesting that distinct and

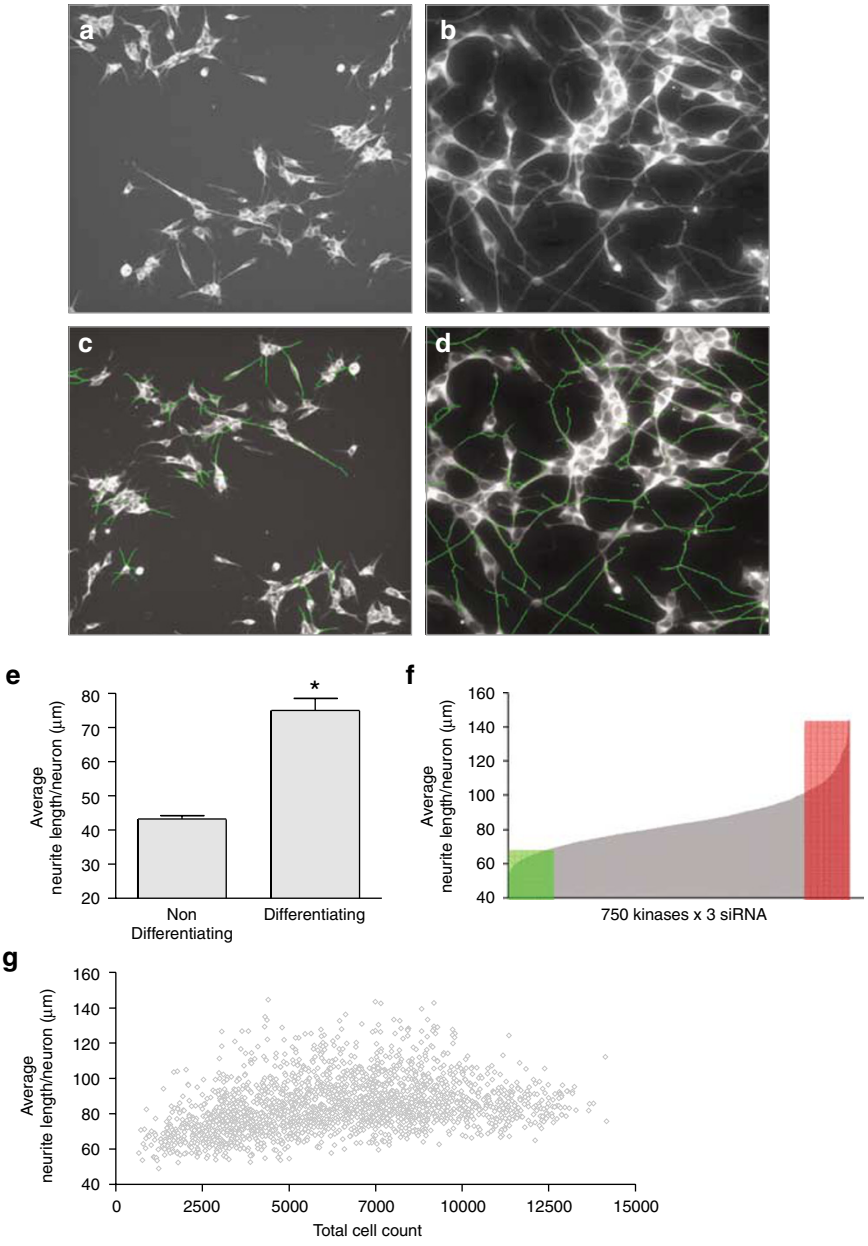

Figure 1 The high throughput neurite outgrowth assay. SH SY-5Y cells were fixed after 48 h in non-differentiating (**a** and **c**) or differentiating (**b** and **d**) medium and immunostained with neuronal-specific marker βIII tubulin. Fluorescence images (with 10 $\times$ magnification) acquired using the Cellomics High Content system (**a** and **b**) and the same images following application of neurite outgrowth algorithm (**c** and **d**). (**e**) A histogram showing the average neurite length/neuron of SH SY-5Y cells in differentiating or non-differentiating medium 48 h post-transfection with scrambled siRNA. Error bars = S.D., $n = 40$ in all groups, $^*P$ value $= 1.98 \times 10^{-35}$ with one tailed *t*-test. (**f**) A histogram showing the average neurite length/neuron of all samples (750 kinases siRNA with three-fold redundancy). Candidates with average neurite length/neuron less than 70 μm and more than 100 μm were highlighted in green and red, respectively. (**g**) A scatter plot showing the distribution of total numbers of neuron acquired and their respective calculated average neurite length per neuron

non-over-lapping signalling mechanisms are responsible for these two processes.

Validation of the screens in primary neurons. To validate the authenticity of our screen results, we selected a subset of siRNA to downregulate kinases in primary cultures of cerebellar granule neurons (CGN). Two independent siRNAs to rat orthologues of six candidates (cdc2a, ulk1, mast2, fastk, pdk1 and map4k4), identified by the promoting outgrowth data set, were co-transfected with a green fluorescent protein (GFP) reporter construct and fluorescence images of siRNA-transfected cultures were acquired 2 days post-transfection (Figure 4a–d). The outgrowth of neuronal processes from GFP-positive neurons was quantified and compared to cultures transfected with scrambled siRNA. The neurite length/neuron values were significantly higher than those with scrambled siRNA control for all CGN cultures (Figure 4).

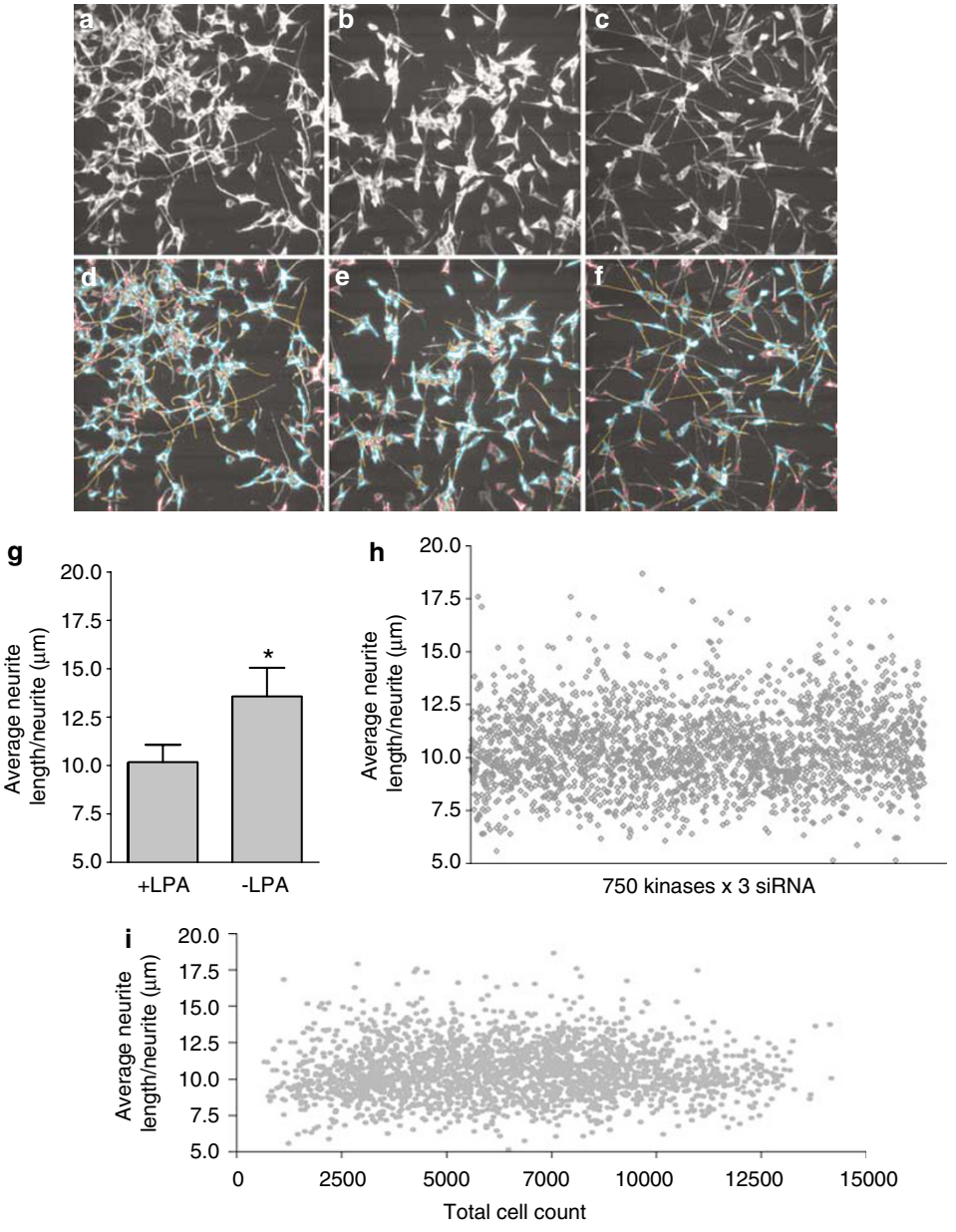

Figure 2 The high throughput neurite retraction assay. SH SY-5Y cells were fixed 48 h post-transfection with scrambled siRNA (**a**, **b**, **d** and **e**) or ROCK1 siRNA (**c** and **f**) in differentiating medium and immunostained with neuronal-specific marker βIII tubulin. Fluorescence images (with $\times 10$ magnification) acquired using the Cellomics High Content system (**a**, **b** and **c**) and the same images following application of extended neurite Outgrowth algorithm (**d**, **e** and **f**). (**g**) A histogram showing the average neurite length/neurite of SH SY-5Y cells in differentiating medium, with or without 10 μM LPA induction, 48 h post-transfection with scrambled siRNA. Error bars = S.D., $n = 104$ in all groups, *P value $= 9.0 \times 10^{-42}$ with one tailed t-test. (**h**) A histogram showing the average neurite length/neurite of all samples (750 kinases siRNA with three-fold redundancy). Candidates with average neurite length/neurite more than 12 μm were defined as inhibiting LPA-induced neurite retraction. (**i**) A scatter plot showing the distribution of total numbers of neuron acquired and their respective calculated average neurite length per neurite

The regeneration data were validated in another subset of kinases using a model of primary dopaminergic neuron regeneration.[26] Axons were transected at day *in vitro* (DIV) 3 and siRNA-transfected cultures were then kept until DIV 6 to allow for regeneration of lesioned axons. Regeneration from the edge of the transection was then quantified and compared to cultures transfected with a control-siRNA-targeting enhanced green fluorescent protein (EGFP), where the length of regenerating neurites was set to 100% (Figure 5b). Regeneration in the overall culture, containing a majority of GABAergic cells and up to 10% dopaminergic neurons, was quantified in phase contrast images. A significant increase in the length of regenerating neurites was observed in cultures treated with siRNAs directed against CKM, FASTK, MAP4K4, ULK1, MAST2 and PDK1 (Figure 5a). The most pronounced effect on neurite regeneration was observed after knockdown of ULK1 ($167 \pm 12\%$), PDK1 ($165 \pm 15\%$) and FASTK ($163 \pm 19\%$)

Table 1 RNAi knockdown inhibits neurite outgrowth

Amblon name	Also known as	Full name	Kinase subgroup	ANL/ neuron	RefSeq Ace
CHEK1		CHK1 checkpoint homolog (*S. pombe*)	CAMK	66.82	NM_001274
MARK3		MAP/microtubule affinity-regulating kinase 3	CAMK	69.19	NM_002376
MGC8407	VACAMKL		CAMK	64.9	NM_024046
SNARK	NuaK2		CAMK	66.76	NM_030952
TRAD	Kalirin	RhoGEF kinase	CAMK	66.67	NM_007064
TRIO		Triple functional domain (PTPRF interacting)	CAMK	69.72	NM_007118
CDK11		cyclin-dependent kinase (CDC2-like) 11	CMGC	66.35	NM_015076
CDK9		cyclin-dependent kinase 9 (CDC2-related kinase)	CMGC	63.85	NM_001261
CLK4		CDC-like kinase 4	CMGC	62.99	NM_020666
PCTK3	PCTAIRE3	PCTAIRE protein kinase 3	CMGC	59.67	NM_002596, NM_212502, NM_212503
ALS2CR2	STLK6	amyotrophic lateral sclerosis 2 (juvenile) chromosome region, candidate 2	STE	66.64	NM_018571
FLJ23074	YSK4	yeast Sps1/ste20-related kinase 4	STE	68.02	NM_025052
LYK5	STLK5		STE	59.89	NM_001003786. NM_001003787. NM_001003788. NM_153335
MAP2K6		mitogen-activated protein kinase kinase 6	STE	61.81	NM_002758. NM_031988
MAP2K7		mitogen-activated protein kinase kinase 7	STE	64.89	NM_005043, NM_145185
MAP3K4		mitogen-activated protein kinase kinase kinase 4	STE	64.29	NM_005922, NM_006724
MAP3K8	COT/TPL2	mitogen-activated protein kinase kinase kinase 8	STE	62.62	NM_005204
MAP4K5	KHS1	mitogen-activated protein kinase kinase kinase kinase 5	STE	64.22	NM_006575. NM_198794
MINK			STE	62.57	NM_015716, NM_153827 NM_170663
OSR1		oxidative-stress responsive 1	STE	66.2	NM_005109
PAK1		p21/Cdc42/Rac1-activated kinase 1 (STE20 homolog, yeast)	STE	66.49	NM_002576
ALK		anaplastic lymphoma kinase (Ki−1)	TK	62.03	NM_004304
AXL		AXL receptor tyrosine kinase	TK	68.19	NM_001699, NM_021913
EPHA1		EphA1	TK	64.93	NM_005232
EPHA2		EphA2	TK	66.98	NM_004431
EPHA3		EphA3	TK	63.09	NM_005233, NM_182644
ERBB2		v-erb-b2 erythroblastic leukemia viral oncogene homolog 2, neuro/ glioblastoma derived oncogene homolog (avian)	TK	63.21	NM_004448
FES		feline sarcoma oncogene	TK	64.86	NM_002005
FGR		Gardner-Rasheed feline sarcoma viral (v-fgr) oncogene homolog	TK	65.32	NM_005248
FLT3		fms-related tyrosine kinase 3	TK	54.55	NM_004119
FLT4		fms-related tyrosine kinase 4	TK	56.31	NM_002020, NM_182925
JAK1		Janus kinase 1 (a protein tyrosine kinase)	TK	62.17	NM_002227
JAK2		Janus kinase 2 (a protein tyrosine kinase)	TK	65.23	NM_004972
NTRK2	TRKB	neurotrophic tyrosine kinase, receptor, type 2	TK	61.08	NM_006180
RET		ret proto-oncogene (multiple endocrine neoplasia and medullary thyroid carcinoma 1, Hirschsprung disease)	TK	58.76	NM_000323, NM_020629, NM_020630, NM_020975
ROR1		receptor tyrosine kinase-like orphan receptor 1	TK	66.96	NM_005012
RYK		RYK receptor-like tyrosine kinase	TK	59.34	NM_002958
STYK1	SURTK106		TK	63.24	NM_018423
ACVR1C	ALK7	activin A receptor, type IC	TKL	65.44	NM_145259
ACVR2	ACTR2	activin A receptor, type II	TKL	68.29	NM_001616
ACVR2B	ACTR2B	activin A receptor, type IIB	TKL	63.32	NM_001106
ACVRL1	ALK1	activin A receptor type II-like 1	TKL	61.16	NM_000020
ANKK1	Sgk288	ankyrin repeat and kinase domain containing 1	TKL	65.86	NM_178510
BRAF	B-RAF	v-raf murine sarcoma viral oncogene homolog B1	TKL	66.95	NM_004333
FLJ34389	MLKL		TKL	61.25	NM_152649
LIMK1		LIM domain kinase 1	TKL	66.8	NM_002314, NM_016735
MAP3K10	MLK4	mitogen-activated protein kinase kinase kinase 10	TKL	65.68	NM_002446
TGFBR2		transforming growth factor, beta receptor II (70/80 kDa)	TKL	62.22	NM_003242
GCKR		mitogen-activated protein kinase kinase kinase 10		67.11	NM_001486
LIM		PDZ and LIM domains		63.58	NM_006457
MAP3K7IP2		mitogen-activated protein kinase kinase kinase 7 interacting protein 2		66.4	NM_015093, NM_145342
MFHAS1		malignant fibrous histiocytoma amplified sequence 1		59.95	NM_004225

Table 1 *(Continued)*

Amblon name	Also known as	Full name	Kinase subgroup	ANL/ neuron	RefSeq Ace
PIK3AP1		phosphoinositide-3-kinase adaptor protein 1		67.84	NM_152309
PIK3CD		phosphoinositide-3-kinase, catalytic, delta polypeptide		63.67	NM_005026
PIK3CG		phosphoinositide-3-kinase, catalytic, gamma polypeptide		66.44	NM_002649
P1K3R2		phosphoinositide-3-kinase, regulatory subunit, polypeptide 2 (p85 beta)		58.94	NM_005027
PRKAB2		protein kinase, AMP-activated. beta 2 non-catalytic subunit		68.89	NM_005399
PRKAR1B		protein kinase, cAMP-dependent, regulatory, type I, beta		68.33	NM_002735
SCAP1		src family associated phosphoprotein 1		68.33	NM_003726

CAMK, calcium/calmodulin-dependent protein kinase; STE, homologs of yeast sterile 7, sterile 11, sterile 20 kinases; TK, tyrosine kinase; TKL, tyrosine kinase-like. The table shows 59 protein kinases with RNAi phenotype of inhibiting neurite outgrowth in our assay condition. These candidates were grouped according to the subgroup classification in the KINOME (http://kinase.com/human/kinome/).[43] ANL/neuron (average neurite length per neuron) represents average neurite length by three (underlined candidates) or two (un-underlined candidates) independent siRNAs calculated from two rounds of screens

Table 2 RNAi knockdown promotes neurite outgrowth

Ambion name	Also known as	Full name	Kinase subgroup	ANL/ neuron	RefSeq Ace
MAST2		microtubule associated serine/threonine kinase 2	AGC	100.19	NM_015112
MASTL		microtubule associated serine/threonine kinase-like	AGC	103.76	NM_032844
PDPK1		3-phosphoinositide dependent protein kinase-1	AGC	102.92	NM 002613, NM_031268
PRKCB1	PKC beta	protein kinase C. beta 1	AGC	115.98	NM_002738, NM_212535
ROCK1		Rho-associated, coiled-coil containing protein kinase 1	AGC	117.25	NM_005406
ROCK2		Rho-associated, coiled-coil containing protein kinase 2	AGC	100.57	NM_004850
RPS6KA4	MSK2	ribosomal protein S6 kinase, 90 kDa, polypeptide 4	AGC	107.56	NM_003942
ADCK2		aarF domain containing kinase 2	ATYPICAL	107.75	NM 052853
AOCK4		aarF domain containing kinase 4	ATYPICAL	159.08	NM_024876
ATR	FRP-1	ataxia telangiectasia and Rad3 related	ATYPICAL	108.09	NM_001184
BCKDK		branched chain ketoacid dehydrogenase kinase	ATYPICAL	106.09	NM_005881
BCR	PHL. D22S662. D22S11.CML. BCR1, ALL	breakpoint cluster region	ATYPICAL	109.59	NM_004327, NM_021574
BRD3		bromodomain containing 3	ATYPICAL	104.05	NM_007371
BRDT		bromodomain. testis-specific	ATYPICAL	114.25	NM_001726, NM_207189
CABC1	ADCK3, LOC56997	chapetone. ABC1 activity of bc1 complex like (*S. pombe*)	ATYPICAL	118.98	NM 020247
FASTK	FAST. FLJ13079		ATYPICAL	112.02	NM_006712, NM_025096
MIDORI	ALPK3. AlphaK3		ATYPICAL	117.84	NM_020778
SMG1		PI-3-kinase-related kinase SMG-1	ATYPICAL	104.14	NM_014006, NM_015092
TAF1		TAF1 RNA polymerase II, TATA box binding protein (TBP)-associated factor. 250 kDa	ATYPICAL	107.91	NM_004606, NM_138923
TAF1L		TAF1-like RNA polymerase II, TATA box binding protein (TBP)-associated factor, 210 kDa	ATYPICAL	128.93	NM_153809
TRPM6	CHAK2	transient receptor potential cation channel, subfamily M, member 6	ATYPICAL	125.54	NM_017662
CDC2	CDK1. p34cdc2	cell division cycle 2, G1 to S and G2 to M	CMGC	118.83	NM_001786, NM_033379
AURKC	AURC, ALK3. AIE2. STK13	aurora kinase C	OTHER	103.1	NM_003160
BUB1		BUB1 budding uninhibited by benzImidazoles 1 homolog (yeast)	OTHER	105.73	NM_004336
CHUK	IKK alpha	conserved helix-loop-helix ubiquitous kinase	OTHER	99.44	NM_001278
CSNK2A2	ck2alpha2	casein kinase 2. alpha prime polypeptide	OTHER	115.26	NM_001896
ERN2	IRE2	ER to nucleus signalling 2	OTHER	113.71	NM_033266
FLJ32685	NEK10		OTHER	140.36	NM_152534
HRI			OTHER	113.38	NM_014413
MOS	c-mos, msv	v-mos Moloney murine sarcoma viral oncogene homolog	OTHER	101.93	NM_005372
NEK11		NIMA (never in mitosis gene a)-related kinase 11	OTHER	110.07	NM_024800, NM_145910
NEK3		NIMA (never in mitosis gene a)-related kinase 3	OTHER	104.06	NM 002498, NM_152720
NEK4		NIMA (never in mitosis gene a)-related kinase 4	OTHER	109.85	NM_003157
NEK6		NIMA (never in mitosis gene a)-related kinase 6	OTHER	105.86	NM_014397
NEK7		NIMA (never in mitosis gene a)-related kinase 7	OTHER	99.36	NM_133494

Table 2 *(Continued)*

Ambion name	Also known as	Full name	Kinase subgroup	ANL/ neuron	RefSeq Ace
PLK4	STK18. SAK	polo-like kinase 4 (*Drosophila*)	OTHER	100.84	NM 014264
PRKWNK2	Wnk2	protein kinase, lysine deficient 2	OTHER	110.63	NM_006648
PRKWNK3	Wnk3	protein kinase, lysine deficient 3	OTHER	106.31	NM_001002838, NM_020922
PTK9L	A6r	PTK9L protein tyrosine kinase 9-like (A6-related protein)	OTHER	117.06	NM 007284
SCYL1	NTKL	SCY1-like 1 (*S. cerevisiae*)	OTHER	102.04	NM_020680
STK35	CLIK1	serine/threonine kinase 35	OTHER	99.83	NM_080836
TBK1		TANK-binding kinase 1	OTHER	118.72	NM_013254
TLK1		tousled-like kinase 1	OTHER	108.42	NM 012290
TOPK	PBK	PDZ binding kinase	OTHER	101.71	NM_018492
TP53RK	PRPK	TP53 regulating kinase	OTHER	109.7	NM_033550
ULK1		unc-51-like kinase 1 (*C. elegans*)	OTHER	123.12	NM_003565
ULK2		unc-51-like kinase 2 (*C. elegans*)	OTHER	111.4	NM 014683
NPR1		natriuretic peptide receptor A/guanylate cyclase A (atrionatriuretic peptide receptor A)	RGC	111.24	NM_000906
MAP4K4	NIK	mitogen-activated protein kinase kinase kinase kinase 4	STE	109.98	NM_004834. NM_145686, NM_145687
MY03B		myosin IIIB	STE	108.34	NM_138995
TA01		Thousand-and one amino acid	STE	108.31	NM 004783, NM_016151
CERK		ceramide kinase		115.91	NM_022766, NM_182661
CKM		creatine kinase, muscle		112.4	NM_001824
CKMT2		creatine kinase, mitochondhal 2 (sarcomeric)		104.76	NM 001825
DCK		deoxycytidine kinase		101	NM_000788
DGKD		diacylglycerol kinase, delta l30 kDa		101.61	NM_003648, NM_152879
DGUOK		deoxyguanosine kinase		100.71	NM_001929, NM_080915, NM_080916, NM_080917. NM 080918
ETNK2		ethanolamine kinase 2		102.67	NM_018208
GALK1		galactokinase 1		107.31	NM_000154
NME3		non-metastatic cells 3, protein expressed in		112.94	NM_002513
PIP5K1A		phosphatidylinositol-4-phosphate 5-kinase. type I, alpha		106.76	NM 003557
P1P5K2A		phosphatidylinositol-4-phosphate 5-kinase. type II, alpha		102.79	NM_005028
PRKRA		protein kinase, interferon-inducible double stranded RNA dependent activator		110.06	NM_003690
TK1		thymidine kinase 1, soluble		106.98	NM_003258
TK2		thymidine kinase 2, mitochondrial		105.58	NM_004614
UCK1		uridine-cytidine kinase 1		108.71	NM_031432

AGC, containing PKA, PKG, PKC families; ATYPICAL, 'atypical' kinases with no sequence similarity to typical kinases but are known or predicted to have enzymatic activity; CMGC, containing CDK, MAPK, GSK3, CLK families; OTHER, the Other group contains several kinase families that do not fit within any of the other main kinase groups; RGC, receptor guanylate cyclases; STE, homologues of yeast sterile 7, sterile 11, sterile 20 kinases. The table shows 66 protein kinases with RNAi phenotype of promoting neurite outgrowth in our assay condition. These candidates were grouped according to the subgroup classification in the KINOME (http://kinase.com/human/kinome/).[43] ANL/neuron (average neurite length per neuron) represents average neurite length by three (underlined candidates) or two (un-underlined candidates) independent siRNAs calculated from two rounds of screens

compared to the anti-EGFP siRNA-treated controls ($100 \pm 8\%$).

To quantify regeneration in the sub-population of dopaminergic neurons in culture, we performed immunocytochemistry for tyrosine hydroxylase (TH) and measured regeneration beyond the edge of the transection as in the total culture (Figure 5d). In general, regeneration of dopaminergic neurons was less pronounced compared to overall regeneration in culture, suggesting a lower regeneration potential of this sub-population (Figure 5c). Increased regeneration of TH-positive neurons was observed with knockdown of DGUOK ($131 \pm 9\%$), MAP4K4 ($124 \pm 6\%$) and ULK1 ($130 \pm 8\%$) compared to the anti-EGFP siRNA-treated control.

Validation in *Drosophila* retinal degeneration. To address the physiological significance of our finding *in vivo*, we tested *Drosophila* orthologues of two candidate kinases essential for neurite retraction, ROCK1 and PKN1, for their ability to influence retinal degeneration in class III Autosomal Dominant *Drosophila* Retinitis Pigmentosa (ADRP). We used two mutant alleles of *Drosophila ninaE* gene, $ninaE^{G69D}$ and $ninaE^{RH27}$, which share molecular and phenotypic characteristics identical to those found in human ADRP.[27,28] Heterozygous *ninaE* flies exhibit age-related retinal degeneration.[28] The severity of degeneration intensified when the animals were reared in permanent light and to a lesser extent when reared in darkness[29] (Figure 6a and b). We tested whether mutant alleles of the fly orthologue

Table 3 RNAi knockdown inhibits LPA-induced neurite retraction

Ambion name	Also known as	Full name	Kinase subgroup	ANL/ neurite	RefSeq Acc
ADRBK1	BARK1/ GRK2	adrenergic, beta, receptor kinase 1	AGC	12.8	NM_001619
AKT1		v-akt murine thymoma viral oncogene homolog 1	AGC	12.65	NM 005163
GRK5	GPRK5	G protein-coupled receptor kinase 5	AGC	14.12	NM_005308
LATS2		LATS, large tumor suppressor, homolog 2 (*Drosophila*)	AGC	13.41	NM_014572
MAST2		microtubule associated serine/threonine kinase 2	AGC	14.6	NM_015112
MASTL		microtubule associated serine/threonine kinase-like	AGC	13.25	NM 032844
PDPK1	PDK1	3-phosphoinositide dependent protein kinase-1	AGC	13.91	NM_002613, NM_031268
PKN1	PRK1	protein kinase N1	AGC	13.3	NM_002741, NM_213560
PRKCB1	PKC beta	protein kinase C, beta 1	AGC	14.68	NM 002738, NM_212535
PRKCG	PKC gamma	protein kinase C, gamma	AGC	13.76	NM_002739
PRKCI	PKC iota	protein kinase C, iota	AGC	14.89	NM_002740
PRKY		protein kinase, Y-linked	AGC	15.12	NM 002760
ROCK1		Rho-associated, coiled-coil containing protein kinase 1	AGC	14.18	NM_005406
STK32B	YANK2	serine/threonine kinase 32B	AGC	13.51	NM_018401
STK38L	NDR2	serine/threonine kinase 38 like	AGC	13.43	NM_015000
ADCK2	CABC1	aarF domain containing kinase 2	ATYPICAL	12.7	NM 052853
ADCK4	CABC1	aarF domain containing kinase 4	ATYPICAL	14.08	NM_024876
CABC1	ADCK3	chaperone, ABC1 activity of bc1 complex like (*S. pombe*)	ATYPICAL	12.62	NM_020247
MIDORI	ALPK3		ATYPICAL	13.73	NM 020778
FASTK			ATYPICAL	12.6	NM_006712, NM_025096
HUNK		hormonally upregulated Neu-associated kinase	CAMK	12.98	NM_014586
KIAA0999	QSK		CAMK	13.71	NM_025164
MKNK2	MNK2	MAP kinase interacting serine/threonine kinase 2	CAMK	14.83	NM 017572, NM_199054
PHKG1		phosphorylase kinase, gamma 1 (muscle)	CAMK	12.63	NM_006213
PSKH2		protein serine kinase H2	CAMK	14.37	NM_033126
STK22D	TSSK1	serine/threonine kinase 22D (spermiogenesis associated)	CAMK	13.7	NM 032028
CDC2	CDK1	cell division cycle 2, G1 to S and G2 to M	CMGC	12.96	NM_001786, NM_033379
HIPK1		homeodomain interacting protein kinase 1	CMGC	13.09	NM_152696, NM_181358, NM_198268, NM_198269
SCYL1		SCY1-like 1 (*S. cerevisiae*)	OTHER	13.1	NM_020680
SGK	CLIK1	serum/glucocorticoid regulated kinase	OTHER	12.72	NM_005627
TBK1		TANK-binding kinase 1	OTHER	12.48	NM 013254
ULK1		unc-51-like kinase 1 (*C. elegans*)	OTHER	14.41	NM_003565
ULK2		unc-51-like kinase 2 (*C. elegans*)	OTHER	12.61	NM_014683
PTK9L		PTK9L protein tyrosine kinase 9-like (A6-related protein)	OTHER	12.93	NM 007284
PAK6		p21(CDKN1A)-activated kinase 6	STE	12.03	NM_020168
SLK		STE20-like kinase (yeast)	STE	13.54	NM_014720
STK10	LOK	serine/threonine kinase 10	STE	13.19	NM_005990.
MAP4K4	HGK/NIK	mitogen-activated protein kinase kinase kinase kinase 4	STE	13.44	NM_004834, NM_145686 NM_145687
EGFR		epidermal growth factor receptor (erythroblastic leukemia viral (v-erb-b) oncogene homolog. avian)	TK	14.83	NM_005228, NM_201282, NM_201283, NM_201284
FGFR1		fibroblast growth factor receptor 1 (fms-related tyrosine kinase 2, Pfeiffer syndrome)	TK	13.35	NM_000604. NM_015850 NM_023105, NM_023106
FGFR4		fibroblast growth factor receptor 4	TK	14.48	NM_002011, NM_022963 NM_213647
FLT1	VEGFR1	fms-related tyrosine kinase 1 (vascular endothelial growth factor/ vascular permeability factor receptor)	TK	13.4	NM_002019
HCK		hemopoietic cell kinase	TK	12.77	NM_002110
LTK		leukocyte tyrosine kinase	TK	13.51	NM 002344, NM_206961
MST1R	RON	macrophage stimulating 1 receptor (c-met-related tyrosine kinase)	TK	13.76	NM_002447
NTRK1	TRKA	neurotrophic tyrosine kinase, receptor, type 1	TK	13.75	NM_002529
NTRK3	TRKC	neurotrophic tyrosine kinase, receptor, type 3	TK	12.28	NM_002530
PPGFRB		platelet-derived growth factor receptor, beta polypeptide	TK	12.22	NM 002609
PTK2B	PYK2	PTK2B protein tyrosine kinase 2 beta	TK	13.01	

Table 3 *(Continued)*

Ambion name	Also known as	Full name	Kinase subgroup	ANL/ neurite	RefSeq Acc
					NM_004103, NM_173174, NM_173175, NM_173176
PTK6	BRK	PTK6 protein tyrosine kinase 6	TK	13.54	NM 005975
PTK7	CCK4	PTK7 protein tyrosine kinase 7	TK	13.83	NM_002821, NM_152880 NM_152881, NM_152882
SRMS	SRM	src-related kinase lacking C-terminal regulatory tyrosine and N-terminal myristylation sites	TK	13.39	NM_080823.
TEC		tec protein tyrosine kinase	TK	14.8	NM_003215,
TYR03	SKY	TYR03 protein tyrosine kinase	TK	13.43	NM_006293
AMHR2	MIAR2	anti-Mullerian hormone receptor, type II	TKL	13.57	NM_020547
ILK		integrin-linked kinase	TKL	13.41	NM 004517
IRAK3		interieukin-I receptor-associated kinase 3	TKL	12.61	NM_007199
CERK		ceramide kinase		14.1	NM_022766, NM_182661
DAB2		disabled homolog 2, mitogen-responsive phosphoprotein (*Drosophila*)		13.39	NM_001343
DGKD		diacylglycerol kinase, delta I30 kDa		12.32	NM_003648, NM_152879
DGKO		diacylglycerol kinase, theta 110 kDa		14.16	NM_001347
FN3KRP		fructosamine-3-kinase-related protein		12.36	NM 024619
GK2		glycerol kinase 2		12.26	NM_033214
IHPK1		inositol hcxaphosphate kinase 1		14.52	NM_153273
NME3		non-metastatic cells 3		12.66	NM 002513
PGK2		phosphoglycerate kinase 2		13.15	NM_138733
PRPS2		phosphoribosyl pyrophosphate synthetase 2		13.92	NM_002765
TSKS		testis-specific kinase substrate		13.11	NM_021733

AGC, containing PKA, PKG, PKC families; ATYPICAL, 'atypical' kinases with no sequence similarity to typical kinases but are known or predicted to have enzymatic activity; CAMK, calcium/calmodulin-dependent protein kinase; CMGC, containing CDK, MAPK, GSK3, CLK families; OTHER, the Other group contains several kinase families that do not fit within any of the other main kinase groups; STE, homologues of yeast sterile 7, sterile 11, sterile 20 kinases; TK, tyrosine kinase; TKL, tyrosine kinase-like. The table shows 79 protein kinases with RNAi phenotype of inhibiting LPA-induced neurite retraction in our assay condition. These candidates were grouped according to the subgroup classification in the KINOME (http://kinase.com/human/kinome/).[43] ANL/neurite (average neurite length per neurite) represents average neurite length by three (underlined candidates) or two (un-underlined candidates) independent siRNAs calculated from two rounds of screens

of human ROCK1, *rok*, could influence light-induced retinal degeneration in *ninaE* flies. Heterozygous *rok* mutant suppressed retinal degeneration in *ninaE* heterozygous background (Figure 6a). We also tested another candidate kinase from the retraction screen, PKN1, using this light-induced retinal degeneration assay. Similarly, heterozygous *pkn* mutant suppressed retinal degeneration in *ninaE* flies, although to a lesser extent than those exhibited by *rok* mutant (Figure 6b).

Discussion

A comprehensive understanding of the molecular modulators and signalling network involved in the processes of axon outgrowth, growth cone collapse, axon retraction and degeneration is fundamental in order to gain insight into the mechanism of neuronal degeneration and regeneration. Our genome-wide screen provides a comprehensive analysis and classification of kinase gene families on the basis of their role in neurite outgrowth and retraction. This study not only places known players of neurite outgrowth and retraction into a wider context, but also identifies a large group of kinases with previously unknown function or kinases not previously implicated in regulation of axonal growth/maintenance.

Our results show that approximately 8 and 9% of the whole KINOME is essential for the promotion and inhibition of neurite outgrowth, respectively. As expected, known kinase regulators of mammalian axonal outgrowth, such as TRKB, and members of the Eph receptor TK family and also kinase proteins essential for neuronal development in lower organisms, such as unc-51 and MINK, were revealed by the screen.[30–33] Similarly, the identification of JAK1 and JAK2 kinases of the JAK/STAT pathway for neurite outgrowth (Table 1) is consistent with a previously described function of STAT3 activation, which is necessary to increase growth of dorsal root ganglion neurons and improve axonal regeneration in spinal cord after a conditioning injury.[34]

Nevertheless, the majority of the candidates, many of which have housekeeping functions such as mitochondrial DNA (mtDNA) synthesis and cell cycle-related kinases (Table 2), have not been described to influence neurite outgrowth. For example, in non-replicating cells such as neurons, where cytosolic deoxyribonucleotide triphosphate synthesis is downregulated, mtDNA synthesis depends solely on the mitochondrial salvage pathway enzymes, deoxyribonucleoside kinases. Intriguingly, RNAi downregulation of all four mammalian deoxyribonucleoside kinases, DCK, TK1, TK2 and DGUOK, promote neurite outgrowth. Mutations in DGUOK and TK2 have been found in patients

with mtDNA depletion syndromes and 10–15% of these patients exhibit neuronal abnormalities.[35] The identification of all deoxyribonucleoside kinases as negative regulators of neurite outgrowth suggests that mtDNA synthesis machinery negatively regulates neurite outgrowth and is essential for neuronal function.

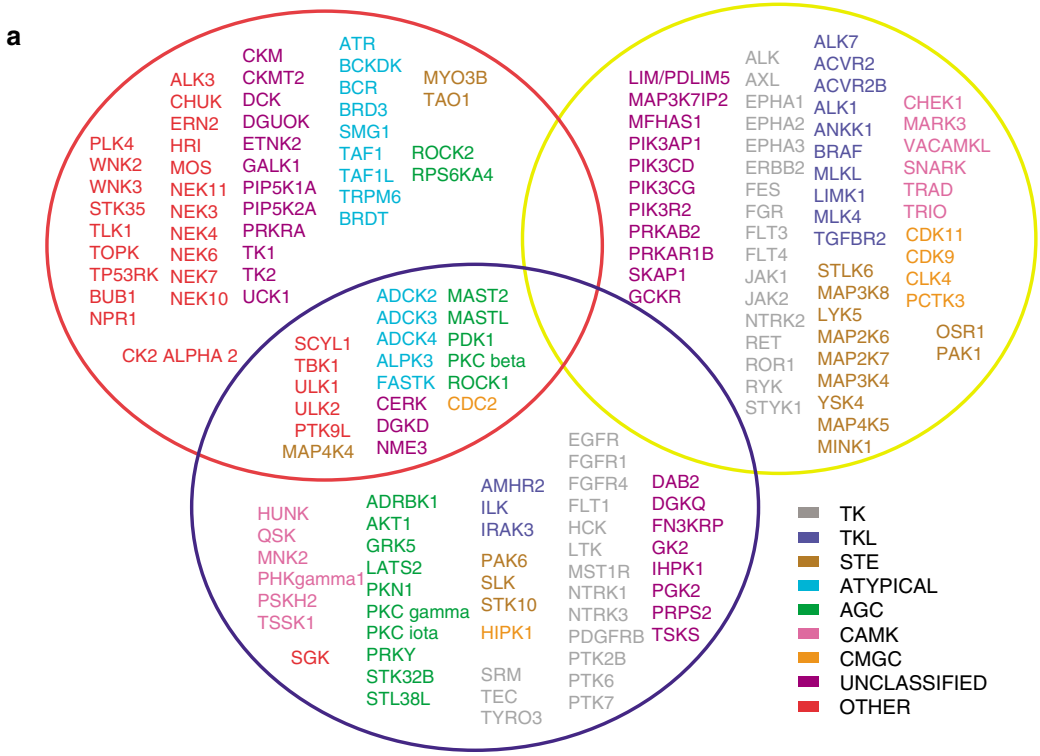

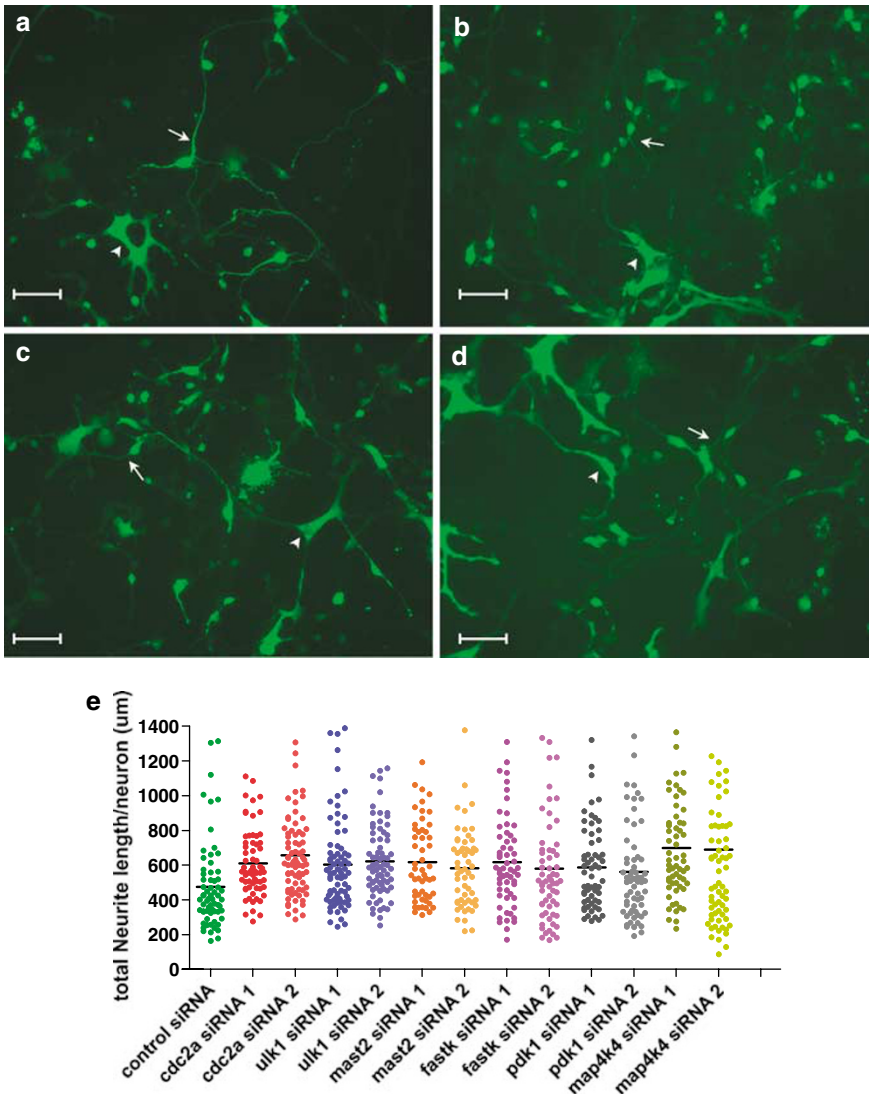

Figure 4 Neurite outgrowth of CGN cultures after siRNA-mediated knockdown. Representative fluorescent images of culture CGN co-transfected with pmaxGFP and scrambled siRNA (**a**) or siRNA-targeting MAST2 (**b**), ULK1 (**c**) and FASTK (**d**). Neurite length was traced on CGN population (arrows) but not on the distinctive larger population of glial cells (arrowhead). Scale bar = 50 μm. (**e**) A scatter plot of total neurite length per neuron for all sample traced. Each dot represents a traced neuron and the black bar represents the average neurite length per neuron (μm) for each sample. siRNA-mediated knock down of selected kinases result in significantly longer total neurite length per neuron than the scramble siRNA, using the two-tailed *t*-test: $P = 0.00039$ (cdc2a siRNA1), $P = 0.000014$ (cdc2a siRNA2), $P = 0.0018$ (ulk1 siRNA1), $P = 0.00013$ (ulk1 siRNA2), $P = 0.00089$ (mast2 siRNA1), $P = 0.007$ (mast2 siRNA2), $P = 0.0011$ (fastk siRNA1), $P = 0.0258$ (fastk siRNA2), $P = 0.0058$ (pdk1 siRNA1), $P = 0.0348$ (pdk1 siRNA2), $P = 0.000005$ (map4k4 siRNA1) and $P = 0.00024$ (map4k4 siRNA2)

Figure 3 Candidate kinases identified in neurite outgrowth and retraction screens. All candidate kinases identified in both the neurite outgrowth and retraction screens are listed. (**a**) A Venn diagram showing RNAi downregulation of candidates in yellow or red circles resulted in inhibition or promotion of neurite outgrowth, respectively. RNAi downregulation of candidates in blue circles inhibits neurite retraction induced by LPA induction. Note that there are overlapping candidates between these data sets. All candidates were colour coded according to their subgroups classification in the KINOME (http://kinase.com/kinbase/). TK, tyrosine kinase in grey; TKL, tyrosine kinase-like in blue; STE, homologues of yeast sterile 7, sterile 11, sterile 20 kinases in brown; ATYPICAL, 'atypical' kinases with no sequence similarity to typical kinases but are known or predicted to have enzymatic activity in turquoise; AGC, containing PKA, PKG, PKC families in green; CAMK, calcium/calmodulin-dependent protein kinase in pink; CMGC, containing CDK, MAPK, GSK3, CLK families in orange; UNCLASSIFIED, candidates present in the library but could not be linked to a particular subgroup in the KINOME in purple; OTHER, the other group contains several kinase families that do not fit within any of the other main kinase groups in red. (**b**) The kinase signalling cross-talk, and connection between different members of kinases families identified in the screens. Links were established between identified kinases using PathwayArchitect^{TM} software (Stratagene). For clarity, the pathway was generated automatically by a proprietary algorithm that finds direct connections between selected candidate kinases within the context of hand-curated and text-mined data present in the database. Candidates with rhombus or ellipse shapes are from the inhibition or promotion list of the outgrowth screen, respectively. Candidates with a rectangular shape are from the list of the inhibition of LPA-induced neurite retraction and those in octagon shape overlapped between promoting list and retraction list. Colour coding of kinases subgroup classification are as in (**a**). Small green squares linking two nodes represent positive or negative regulation as indicated. Small blue squares and orange circles represent binding interaction and protein modification between two nodes, respectively

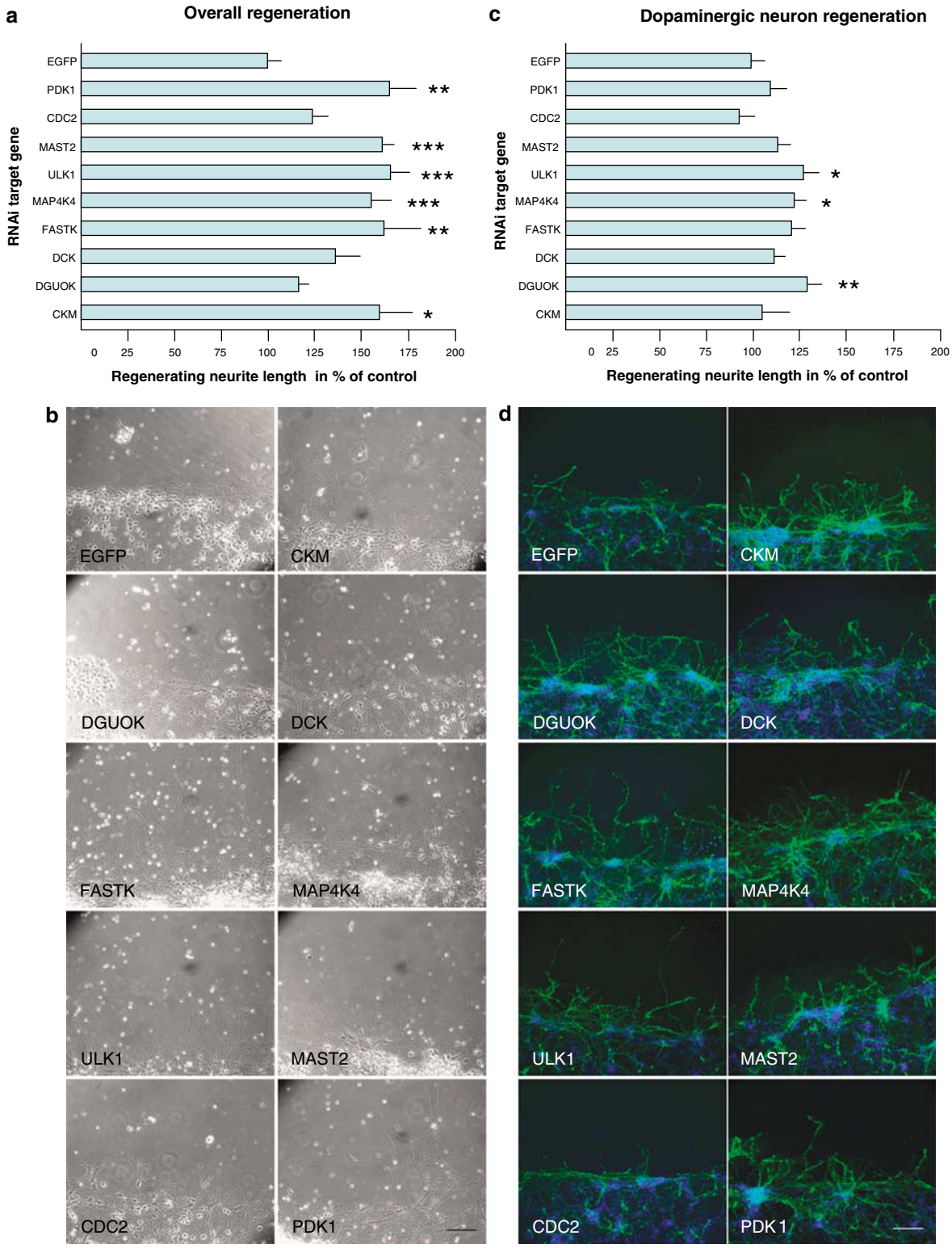

Figure 5 Regeneration of primary midbrain neurons after RNAi-induced knockdown. Bar diagrams represent quantification of neurite regeneration beyond the scratch lesion in the total knockdown culture given in percent compared to cultures treated with anti-EGFP siRNA; (**a**) regeneration in total culture, (**c**) regeneration in the dopaminergic sub-population. Data are given as mean $\pm$ S.E.M. Neurite lengths were considered significantly different at $^{*}P<0.05$, $^{**}P<0.01$ and $^{***}P<0.001$ according to a two-sided *t*-test compared with the anti-EGFP siRNA-treated control. Photomicrographs: representative phase contrast (**b**) or epifluorescence images (**d**; blue – DAPI, green – TH) displaying regenerating neurites beyond the scratch lesion in cultures treated with siRNA against selected kinases or EGFP. Bar: 100 μm

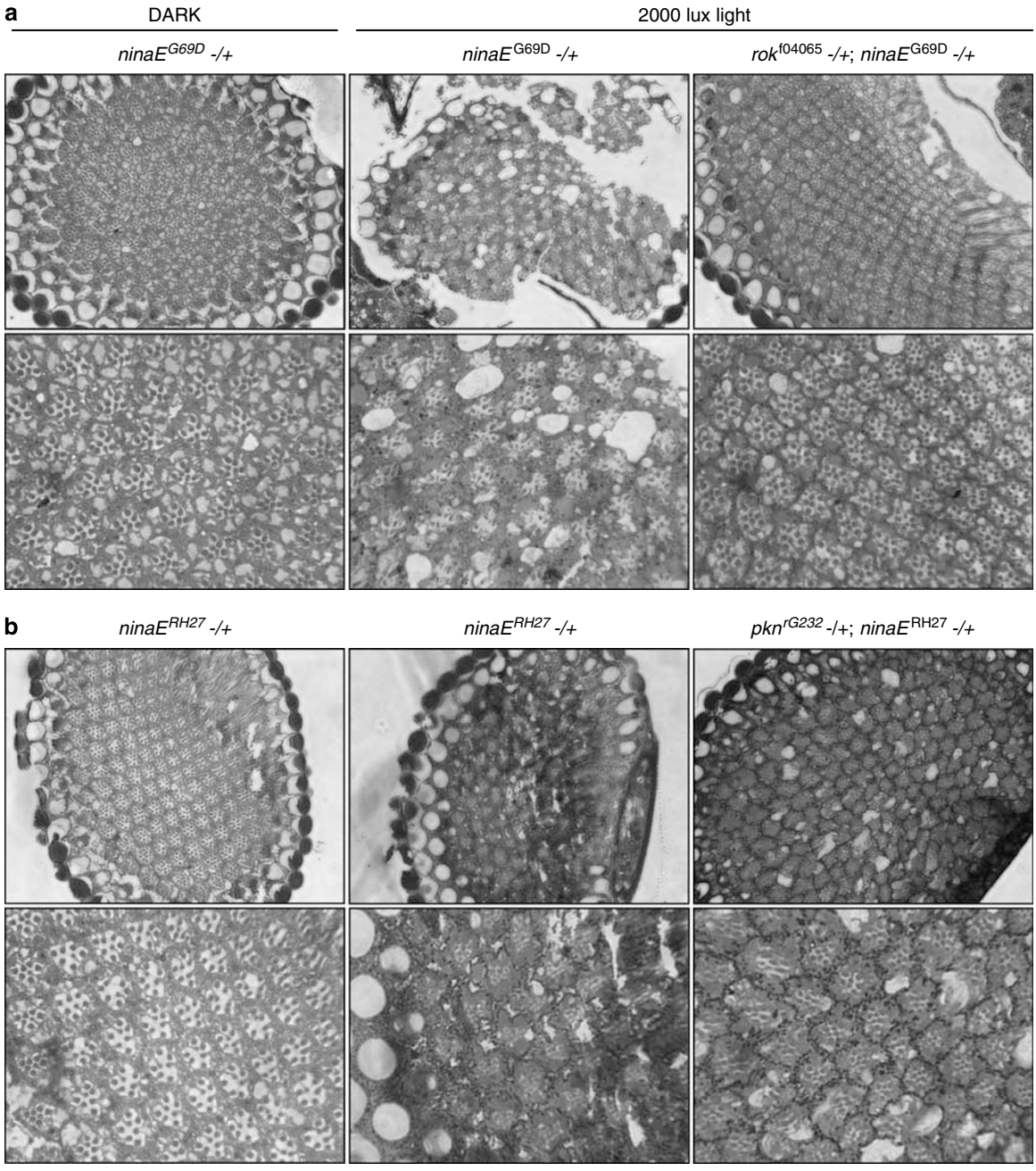

Figure 6 Haploinsufficiency of ROK and PKN1 suppressed ninaE$-/+$ retinal degeneration. Light micrographs of retinal tangential sections of flies: (**a**) *ninaE*$^{G69D}-/+$, *rok*$^{f04065}-/+$; *ninaE*$^{G69D}-/+$; (**b**) *ninaE*$^{RH27}-/+$, *pkn*$^{rG232}-/+$; *ninaE*$^{RH27}-/+$ raised in constant darkness or constant light (2000 lux) for 4 weeks. Light-induced retinal degeneration in two genetic backgrounds of *ninaE* mutations, *ninaE*^{G69D} and *ninaE*^{RH27} were suppressed by haploinsufficiency of ROK (*rok*^{f04065}) and PKN (*pkn*^{rG232}). Upper panels of both (**a**) and (**b**) are $\times 40$ magnification, whereas the lower panels are of $\times 100$ magnification

Cell cycle exit represents the fundamental step to trigger differentiation of cells. It is therefore not surprising that downregulation of check point kinases, such as CHEK1, CDK11, CDK9 and CLK4, led to inhibition of neurite outgrowth (Table 1). These cannot be formally validated as direct modulators of axodendritic length, without testing their role in non-dividing cells. On the other hand, downregulation of a subset of cell cycle kinases, BUB1, AURKC, PLK4 and members of the NEK kinase family, promotes the outgrowth of neurites in our assay condition, suggesting that functions unrelated to cell cycle progression are modulated by these proteins. Indeed, recent convergence of data indicates a relationship between cilia, cell size and cell cycle progression.[36] Based on our screen results, it is conceivable that signalling pathways regulating cytoskeletal rearrangement may be similar for both cell cycle progression and neurite outgrowth, and that the so-called cell cycle kinases may have a wider role.

Finally, our outgrowth screen also identified CKM and CKMT2, two major isozymes of creatine kinase, as negative regulators of neurite outgrowth. The importance of these kinases as negative regulators of neurite outgrowth is further confirmed by the dopaminergic neuronal culture regeneration model (Figure 5). Supplementation of the substrate of this kinase, creatine, has been shown to protect neurons against neurotoxins *in vitro* and was able to slow down the progression of a number of neurodegenerative disease states in experimental animal models.[37,38] Our finding further highlights the role of creatine kinase in neuroprotection and as a putative target for drugs aimed to promote neuronal regeneration and inhibit neuronal degeneration.

LPA-induced neurite retraction involves Rho GTPase signalling and ROCK1, which is a well-characterized mediator of neurite regression.[25,39] ROCK is crucial for mediating the growth inhibitory signal of myelin proteins in the CNS and its inhibition has been shown to increase axonal regeneration *in vivo.*[40] In addition to ROCK1, a series of kinases previously unrelated to neurite degeneration was identified by the screen (Table 3). Among others, PI3K (via AKT and PKC) and cytoplasmic and receptor TK signalling (EGFR, FGFR, PDGFR and FLT1) were essential for LPA-induced neurite retraction. To validate both known and novel kinases revealed by the screen, we selected ROCK1 and a member of the PKC superfamily, PKN1. Haploinsufficiency of either *rok*, a *Drosophila* orthologue of human ROCK1, or PKN1 was able to suppress light-induced retinal degeneration in the fly model of ADRP.

Interestingly, 20 candidate kinases shared the property of negative modulators of neurite outgrowth as well as positive modulators of LPA-induced neurite retraction (Table 3). The integrity of the cytoskeleton is essential for the maintenance of axon stability, and axonal retraction requires intimate interaction between actin and microtubule cytoskeleton.[41] It is likely that this subset of kinases is involved in the signalling pathways of the stabilization or destabilization of microtubules, actin or interactions between the two cytoskeletal systems.

The observation of subgroup clustering for all candidates in both screens suggests a different role for different kinase subgroups in neuronal development. For example, members of the AGC, OTHER and ATYPICAL subgroups were predominantly negative modulators of neurite outgrowth and retraction, whereas those of the TK, TKL and STE subgroups were predominantly positive modulators of neurite outgrowth (Figure 3). In addition, clustering of different kinase subgroups (Figure 3b and Supplementary Figure 4) suggests that complex networks involving apparently unrelated groups of kinases are required for neuronal differentiation, degeneration and regeneration. The study of Figure 3b and Supplementary Figure 4 also suggests that complex processes such as neurite length regulation are poorly described by classical, hierarchically arranged, vertical pathways.

This study is far from being an in-depth analysis of all kinases involved in the regulation of neurite length, but provides the first overall picture of the complex signalling network that involves different kinase families in neurite outgrowth and the opposite process of neurite retraction. It also identifies new putative cross-talks between previously unrelated signalling pathways. The mechanisms involved in degeneration of neuronal bodies and their processes, axons and dendrites, involve spatial and temporal signal segregation.[4] The results of this screen are a template for further studies aimed to understand the molecular interaction leading to degeneration/outgrowth of neuronal processes and will help selection of appropriate targets for the design of new therapeutic strategies in neurodegenerative conditions. Protection of axonal and dendritic degeneration and stimulation of the regenerative capacity in damaged neurons might be the best option to improve clinical outcome in human neurodegenerative disorders.

Materials and Methods

siRNA library. A custom siRNA library targeting 750 human kinases with threefold redundancy was obtained from Ambion Inc. The three siRNA duplexes for each target were individually arrayed in a 96-well format (Supplementary Figure 1). Using Fam-labelled siRNA-targeting ROCKII, greater than 92% transfection efficiency was observed (Supplementary Figure 2) and, on average, greater than 66% 'knockdown' for each mRNA target species was observed (Supplementary Figure 3).

High-throughput neurite outgrowth and retraction assays. SH-SY5Y cells were seeded on 96-well plates, at density of 10 000 cells per well, in non-differentiating medium (DMEM with 10% FCS plus 1%P/S) and cultured overnight at 37°C. 24 h post-seeding, non-differentiating medium was replaced with differentiating medium (Neurobasal medium (Invitrogen) supplemented with B27 supplement (Invitrogen), 1%v/v Glutamine and 1 mM db-cAMP (Sigma)) and the cells were transfected with 50 nM siRNA using Lipofectamine 2000 reagent (Invitrogen). Forty-eight hours post-transfection, the cells were fixed with 3% paraformaldehyde in phosphate-buffered saline (PBS) for 20 min at room temperature (RT) followed by treatment for 5 min with 0.1% Triton-X-100 and 50% normal goat serum (NGS) in PBS for 1 h at RT. Neuronal-specific anti-βIII tubulin antibody (Promega) was used to stain the neurite processes at a dilution of 1 in 5000 in 50% NGS at RT for 3–4 h or 4°C overnight with low constant agitation. Bound antibody and nucleus were visualized using Alexa 546-conjugated secondary antibodies (Molecular Probe, 1 in 500) and Hoechst 33342 (Molecular Probe, 1 in 1000), respectively. Retraction assay was identical to the outgrowth assay as mentioned above, except for the addition of 10 μM LPA (Sigma) for an hour before fixing the cells.

Automated images analysis. Cells were imaged using a Cellomics Kinetic Scan Reader high content microscope system and analysed using neurite outgrowth and extended neurite outgrowth BioApplications for the outgrowth and retraction assays, respectively. Twenty images per well per sample were taken at $\times$ 10 magnification in a fully automated and blind manner. The total number of cell counts and the average neurite length per neuron and average neurite length per neurite for duplicated experiments were determined for neurite outgrowth and retraction assays, respectively.

CGNs culture and siRNA transfection. CGNs were prepared from 7-day-old Wistar rat pups and cultured in BME medium (Invitrogen) supplemented with 10% FCS, 25 mM KCl, 1% Glutamax and 1% P/S. Delivery of siRNA into CGNs was performed using the Amaxa nucleofection system (Amaxa GmbH). Optimization was performed with the Amaxa RNAi test kit using pmaxGFP^{TM} plasmid and siRNA directed against pmaxGFP. Following optimization, 6 million cells were co-nucleofected with pmaxGFP and either scrambled siRNA control or gene-specific siRNAs (Qiagen) at a final concentration of 50 nM. Nucleofected cells were plated on poly-L-lysine coated six-well plates and 48 h post-nucleofection cells were fixed with 3% paraformaldehyde. A minimum of 30 images of GFP-positive CGNs was acquired randomly from each well at $\times$ 20 magnification using a Zeiss Axiovert 40 fluorescence microscope. The length of all neurite processes of at least 85 neurons per sample were traced using NeuronJ 1.01 imaging software (Erik Meijering) by two independent researchers. The total neurite length/neuron (μm) was calculated and plotted as scatter plot for all samples traced. The data were analysed by using Student's *t*-test compared to scrambled siRNA control and differences were considered to be significant from $P<0.05$.

***In vitro* regeneration assay and quantitative analysis of axonal regeneration.** Primary midbrain cultures were prepared from embryonic rats on day 14 of gestation (E14) as previously described[26] and maintained in DMEM-F12 (Invitrogen) supplemented with 2.5 mg/ml BSA (35%), 0.9% D-(+)-glucose solution (45%), 2 mM L-glutamine (PAA Laboratories, Pasching, Austria), 5 μg/ml insulin, 1 : 100 N1 medium supplement and 1 : 100 PSN antibiotic mixture (Invitrogen). Half of the culture medium was exchanged at DIV 1 and subsequently every second day. Delivery of siRNA into CGNs was performed using the Amaxa nucleofection system (Amaxa GmbH). Two million cells were nucleoporated with a pool of two gene-specific siRNAs (Qiagen) at a final concentration of 200 nM. Nucleoporated cells were plated on poly-L-ornithine/laminin-coated coverslips in 24-well plates at a density of 5×10^5 cells per well. On DIV 3, a close neurital network was established in culture. A scratch was performed on the surface of the glass coverslip using a 2 mm thick rubber scraper resulting in a lesion on which axonal regeneration could be studied. Each coverslip was microscopically examined to ensure completeness of the scratch. To assess overall neurite outgrowth into the scratch, eight live images per condition were acquired at a random location along the scratch on DIV 6 using an inverted microscope (Axiovert 200 M; Carl Zeiss, Göttingen, Germany). To specifically quantify regeneration of dopaminergic neurons into the scratch, the culture was fixed with 4% paraformaldehyde for 10 min at RT followed by permeabilizing with 100% acetone for 10 min at −20°C and blocking with 10% NGS in PBS for 10 min at RT. Anti-TH antibody (Advanced ImmunoChemical, Long Beach, USA) was used to stain for TH at a dilution of 1 : 250 in 10% NGS overnight at 4°C. Bound antibody and nucleus were visualized using Cy2-conjugated goat anti-rabbit secondary antibody (Abcam, Cambridge, UK) and 4′,6-diamidino-2-phenylindole (DAPI), respectively. Eight images per condition were captured. Quantification of the length of regenerating neurites was performed with the NeuronJ plug-in of the ImageJ software. In each image, the 10 longest processes were measured and averaged. For statistical analysis, all cell culture experiments were repeated at least twice.

***Drosophila* retinal degeneration assay.** The following genotypes were used in this study: *ninaE*^{G69D} and *ninaE*^{RH27} were used as models for the class III ADRP,[27–28] *PKN*^{rG232}*/Cyo*, *PKN*^{k11209}*/Cyo*, *rok*[1]*/FM7i*, *rok*[2]*/FM7i* and *rok[f04065]/FM7i* were from Bloomington stock center. Fly stocks were maintained on standard cornmeal agar media at 25°C in 12 h daylight and 12 h darkness. For light-induced retinal degeneration assay, 20–30 flies with the relevant genotypes were selected and cultured in glass vials at 25°C in permanent light (around 2000 lux) or darkness for 4 weeks. The vials were changed frequently to avoid mixing of the flies with eventual progeny. Tangential plastic sections were performed as previously described,[42] and toluidine blue was used as a dye to increase the contrast.

Acknowledgements. We thank Veronique Planchamp and Anja Krauss for assistance in dopaminergic regeneration assay, Roger Snowdon for assistance in FACS analysis and high throughput screening, Maria Guerra Martin for preparation of CGN cultures, Pedro Domingos (HHMI, The Rockefeller University) and Bloomington Stock Center for fly strains, the Kyriacou lab members for technical assistance in fly work, David Dinsdale, Judy McWilliams and Tim Smith for assistance with TEM, Paul Glynn for critical paper review and Shu Dong Zhang for assistance with statistical analysis.

1. Yuan J, Lipinski M, Degterev A. Diversity in the mechanisms of neuronal cell death. *Neuron* 2003; **40**: 401–413.
2. Finn JT, Weil M, Archer F, Siman R, Srinivasan A, Raff MC. Evidence that Wallerian degeneration and localized axon degeneration induced by local neurotrophin deprivation do not involve caspases. *J Neurosci* 2000; **20**: 1333–1341.
3. Raff MC, Whitmore AV, Finn JT. Axonal self-destruction and neurodegeneration. *Science* 2002; **296**: 868–871.
4. Berliocchi L, Fava E, Leist M, Horvat V, Dinsdale D, Read D *et al.* Botulinum neurotoxin C initiates two different programs for neurite degeneration and neuronal apoptosis. *J Cell Biol* 2005; **168**: 607–618.
5. Dent EW, Gertler FB. Cytoskeletal dynamics and transport in growth cone motility and axon guidance. *Neuron* 2003; **40**: 209–227.
6. Yoshimura T, Arimura N, Kaibuchi K. Signaling networks in neuronal polarization. *J Neurosci* 2006; **26**: 10626–10630.
7. Dancey J, Sausville EA. Issues and progress with protein kinase inhibitors for cancer treatment. *Nat Rev Drug Discov* 2003; **2**: 296–313.
8. Melnikova I, Golden J. Targeting protein kinases. *Nat Rev Drug Discov* 2004; **3**: 993–994.
9. Smith PD, O'Hare MJ, Park DS. Emerging pathogenic role for cyclin dependent kinases in neurodegeneration. *Cell Cycle* 2004; **3**: 289–291.
10. Angelo M, Plattner F, Giese KP. Cyclin-dependent kinase 5 in synaptic plasticity, learning and memory. *J Neurochem* 2006; **99**: 353–370.
11. Lucas JJ, Hernandez F, Gomez-Ramos P, Moran MA, Hen R, Avila J. Decreased nuclear beta-catenin, tau hyperphosphorylation and neurodegeneration in GSK-3beta conditional transgenic mice. *EMBO J* 2001; **20**: 27–39.
12. Hatano Y, Li Y, Sato K, Asakawa S, Yamamura Y, Tomiyama H *et al.* Novel PINK1 mutations in early-onset parkinsonism. *Ann Neurol* 2004; **56**: 424–427.
13. Valente EM, Abou-Sleiman PM, Caputo V, Muqit MM, Harvey K, Gispert S *et al.* Hereditary early-onset Parkinson's disease caused by mutations in PINK1. *Science* 2004; **304**: 1158–1160.
14. Klein C, Schlossmacher MG. The genetics of Parkinson disease: implications for neurological care. *Nat Clin Pract Neurol* 2006; **2**: 136–146.
15. Paisan-Ruiz C, Jain S, Evans EW, Gilks WP, Simon J, van der Brug M *et al.* Cloning of the gene containing mutations that cause PARK8-linked Parkinson's disease. *Neuron* 2004; **44**: 595–600.
16. Zimprich A, Biskup S, Leitner P, Lichtner P, Farrer M, Lincoln S *et al.* Mutations in LRRK2 cause autosomal-dominant parkinsonism with pleomorphic pathology. *Neuron* 2004; **44**: 601–607.
17. Park J, Lee SB, Lee S, Kim Y, Song S, Kim S *et al.* Mitochondrial dysfunction in *Drosophila* PINK1 mutants is complemented by parkin. *Nature* 2006; **441**: 1157–1161.
18. Petit A, Kawarai T, Paitel E, Sanjo N, Maj M, Scheid M *et al.* Wild-type PINK1 prevents basal and induced neuronal apoptosis, a protective effect abrogated by Parkinson disease-related mutations. *J Biol Chem* 2005; **280**: 34025–34032.
19. Gloeckner CJ, Kinkl N, Schumacher A, Braun RJ, O'Neill E, Meitinger T *et al.* The Parkinson disease causing LRRK2 mutation I2020T is associated with increased kinase activity. *Hum Mol Genet* 2006; **15**: 223–232.
20. West AB, Moore DJ, Biskup S, Bugayenko A, Smith WW, Ross CA *et al.* Parkinson's disease-associated mutations in leucine-rich repeat kinase 2 augment kinase activity. *Proc Natl Acad Sci USA* 2005; **102**: 16842–16847.
21. Smith WW, Pei Z, Jiang H, Moore DJ, Liang Y, West AB *et al.* Leucine-rich repeat kinase 2 (LRRK2) interacts with parkin, and mutant LRRK2 induces neuronal degeneration. *Proc Natl Acad Sci USA* 2005; **102**: 18676–18681.
22. Smith WW, Pei Z, Jiang H, Dawson VL, Dawson TM, Ross CA. Kinase activity of mutant LRRK2 mediates neuronal toxicity. *Nat Neurosci* 2006; **9**: 1231–1233.
23. Branchi I, Bichler Z, Minghetti L, Delabar JM, Malchiodi-Albedi F, Gonzalez MC *et al.* Transgenic mouse *in vivo* library of human Down syndrome critical region 1: association between DYRK1A overexpression, brain development abnormalities, and cell cycle protein alteration. *J Neuropathol Exp Neurol* 2004; **63**: 429–440.
24. Lee G, Tanaka M, Park K, Lee SS, Kim YM, Junn E *et al.* Casein kinase II-mediated phosphorylation regulates alpha-synuclein/synphilin-1 interaction and inclusion body formation. *J Biol Chem* 2004; **279**: 6834–6839.
25. Katoh H, Aoki J, Ichikawa A, Negishi M. p160 RhoA-binding kinase ROKalpha induces neurite retraction. *J Biol Chem* 1998; **273**: 2489–2492.
26. Lingor P, Unsicker K, Krieglstein K. GDNF and NT-4 protect midbrain dopaminergic neurons from toxic damage by iron and nitric oxide. *Exp Neurol* 2000; **163**: 55–62.
27. Colley NJ, Cassill JA, Baker EK, Zuker CS. Defective intracellular transport is the molecular basis of rhodopsin-dependent dominant retinal degeneration. *Proc Natl Acad Sci USA* 1995; **92**: 3070–3074.
28. Kurada P, O'Tousa JE. Retinal degeneration caused by dominant rhodopsin mutations in *Drosophila*. *Neuron* 1995; **14**: 571–579.
29. Davidson FF, Steller H. Blocking apoptosis prevents blindness in *Drosophila* retinal degeneration mutants. *Nature* 1998; **391**: 587–591.
30. Poinat P, De Arcangelis A, Sookhareea S, Zhu X, Hedgecock EM, Labouesse M *et al.* A conserved interaction between beta1 integrin/PAT-3 and Nck-interacting kinase/MIG-15 that mediates commissural axon navigation in *C elegans*. *Curr Biol* 2002; **12**: 622–631.
31. Tomoda T, Kim JH, Zhan C, Hatten ME. Role of Unc51.1 and its binding partners in CNS axon outgrowth. *Genes Dev* 2004; **18**: 541–558.
32. Minichiello L, Casagranda F, Tatche RS, Stucky CL, Postigo A, Lewin GR *et al.* Point mutation in trkB causes loss of NT4-dependent neurons without major effects on diverse BDNF responses. *Neuron* 1998; **21**: 335–345.
33. Murai KK, Pasquale EB. New exchanges in eph-dependent growth cone dynamics. *Neuron* 2005; **46**: 161–163.
34. Qiu J, Cafferty WB, McMahon SB, Thompson SW. Conditioning injury-induced spinal axon regeneration requires signal transducer and activator of transcription 3 activation. *J Neurosci* 2005; **25**: 1645–1653.
35. Spinazzola A, Zeviani M. Disorders of nuclear-mitochondrial intergenomic signaling. *Gene* 2005; **354**: 162–168.
36. Quarmby LM, Parker JD. Cilia and the cell cycle? *J Cell Biol* 2005; **169**: 707–710.
37. Ferrante RJ, Andreassen OA, Jenkins BG, Dedeoglu A, Kuemmerle S, Kubilus JK *et al.* Neuroprotective effects of creatine in a transgenic mouse model of Huntington's disease. *J Neurosci* 2000; **20**: 4389–4397.

38. Brewer GJ, Wallimann TW. Protective effect of the energy precursor creatine against toxicity of glutamate and beta-amyloid in rat hippocampal neurons. *J Neurochem* 2000; **74**: 1968–1978.
39. Fukushima N. LPA in neural cell development. *J Cell Biochem* 2004; **92**: 993–1003.
40. Lingor P, Teusch N, Schwarz K, Mueller R, Mack H, Bahr M *et al*. Inhibition of Rho kinase (ROCK) increases neurite outgrowth on chondroitin sulphate proteoglycan *in vitro* and axonal regeneration in the adult optic nerve *in vivo*. *J Neurochem* 2007; **103**: 181–189.
41. Ahmad FJ, Hughey J, Wittmann T, Hyman A, Greaser M, Baas PW. Motor proteins regulate force interactions between microtubules and microfilaments in the axon. *Nat Cell Biol* 2000; **2**: 276–280.
42. Tomlinson A. The cellular dynamics of pattern formation in the eye of *Drosophila*. *J Embryol Exp Morphol* 1985; **89**: 313–331.
43. Manning G, Whyte DB, Martinez R, Hunter T, Sudarsanam S. The protein kinase complement of the human genome. *Science* 2002; **298**: 1912–1934.

Supplementary Information accompanies the paper on Cell Death and Differentiation website (http://www.nature.com/cdd)